DOI:10.1190/segam2021-3582747.1

4D FWI using towed-streamer data: A case study near Laverda oil field

Nanxin Li, Ziqin Yu, Robert To, Min Wang, Yi Xie (CGG), and David Dickinson (Woodside)*

Summary

Time-lapse (4D) seismic surveys are devised to detect subsurface changes resulting from hydrocarbon production and fluid injection. Full-waveform inversion (FWI) of time-lapse seismic data has been reported to provide high-resolution estimates of 4D changes. However, successful applications of 4D FWI on field data have only been seen in a few surveys, either with high repeatability or with large velocity changes. We propose a new workflow to tackle some challenges in 4D FWI, such as cycle-skipping and amplitude mismatch between modeled synthetic data and recorded field data and water-layer variations between baseline and monitor surveys. We applied this approach to a 4D towed-streamer survey in the Exmouth basin, Western Australia. The resulting 4D signals from the direct FWI velocity difference accurately detected softening and hardening effects with changes as low as 1.5% in the reservoir and matched with production history. In addition, the 4D noise was significantly reduced below the reservoirs when the respective baseline and monitor velocity models from 4D FWI were used to migrate baseline and monitor data.

Introduction

Time-lapse (4D) seismic monitoring is widely used in reservoir management in the oil industry to obtain information about reservoir changes. Full-waveform inversion (FWI) was proposed by Lailly (1983) and Tarantola (1984) as an inversion method for automatically building the Earth model. After more than thirty years of development, it is now applied in most 3D seismic imaging projects to establish detailed velocity models. It is a natural thought to combine time-lapse seismic and FWI.

The potential benefits of combining time-lapse seismic and FWI (4D FWI) can be multifold:

- FWI can directly extract physical properties of the subsurface, which are more interpretable than indirect measurements such as image time shift or time strain in normal 4D processing.
- 4D FWI delivers separate velocity models for each survey and therefore allows us to correctly image all vintages. By contrast, conventional 4D to date has generally used the same migration velocity for all vintages combined with a data-driven time-shift correction, which is error prone and imprecise (Macbeth et al., 2018).
- As a byproduct of high-frequency FWI, FWI Imaging (Zhang et al., 2020) has emerged and provided alternative, and sometimes improved, images compared to conventional migration, without tedious preprocessing steps. Using FWI Imaging in time-lapse seismic could bypass preprocessing and provide more rapid turnaround to support reservoir management decisions (Kalinicheva et al., 2020).
- FWI uses not only primary reflections, but also multiples, transmission waves, and diving waves as signals. Thus, it can improve the subsurface illumination compared to primary reflection migration. In conventional 4D projects, the target areas are often close to surface or subsea infrastructure and thus have poor 4D quality due to acquisition holes. 4D FWI could help to illuminate these areas.

However, despite these potential benefits and the recent advancements of 3D FWI, 4D FWI application has remained quite limited. Successful attempts on field data so far are either in highly repeatable acquisitions, such as permanent reservoir monitoring (Hicks et al., 2016; Kamei and Lumley, 2017), OBS (Yang et al., 2015), or in reservoirs with remarkably large velocity changes of around 20% (Maharramov et al., 2019).

Why does 4D FWI not share the same success as well established conventional 4D processing? After investigating the underlying challenges in time-lapse FWI, we identified several key obstacles and propose our corresponding solutions. Finally, we will show a successful application of 4D FWI on a towed-streamer data set near the Laverda oil field in the Exmouth basin.

More robust FWI algorithm

A literature review of 4D FWI shows that choosing the optimal initial model suitable for both the baseline and monitor data is a key concern and has resulted in several 4D FWI schemes. The most straightforward method is to independently invert the models for baseline and monitor using a common initial model. But this approach risks the inversions falling into different local minima due to cycle skipping. The subtraction of such FWI results will be contaminated by 4D artifacts that could easily mask weak 4D signals. Therefore, Hicks et al. (2016) propose to feed both baseline and monitor data sets into FWI to generate an initial model before baseline and monitor parallel inversions. Routh et al. (2012) and Kamei and Lumley (2017) propose a sequential bootstrap approach by first inverting the baseline, then using the baseline FWI model as the initial model for the monitor's inversion. Zhou and Lumley (2019) propose a

DOI:10.1190/segam2021-3582747.1

two-step inversion with crossing initial models between baseline and monitor in the second step.

Even with these improved 4D FWI schemes, the convergence to a true 4D difference is not guaranteed. FWI in the industry is usually acoustic, which has an inherent amplitude mismatch with real data due to the over-simplified physics. When the mismatch between synthetic data and real data is of the same order or bigger than production induced differences, 4D FWI struggles to reveal the time-varying changes.

Zhang et al. (2018) propose a more robust FWI algorithm, i.e., Time-Lag FWI (TLFWI), which focuses on minimizing the discrepancy in traveltimes between synthetic and recorded data. It has more tolerance of the initial model than conventional FWI (Wang et al., 2019). It is also less sensitive to the inherent amplitude differences caused by elastic effects. This suggests that TLFWI is well suited to overcome the issues in current 4D FWI workflows. With the help of TLFWI, amplitude differences related to P-wave and/or S-wave impedance changes will be better decoupled from velocity changes and be more suitable for 4D interpretation.

Handling water-layer variations in FWI

It is well known that in a dedicated 4D acquisition, changing environmental conditions, such as water velocity and tidal height, are dominant non-repeatable factors. It is crucial in conventional 4D processing to estimate and correct these variations in the water layer.

4D FWI uses all wave modes and therefore is more affected by these variations compared to a conventional 4D workflow where only primary reflections are used. For example, peg-leg multiples, which have more passes in the water layer than primary reflections, are more severely impacted by changes in water velocity and tidal height. And these changes cannot be corrected by conventional methods used in standard 4D processing as they are only suitable for primary reflections.

In order to tackle water-layer variations in 4D FWI, we propose a Water-Layer Variant FWI. It is composed of two steps. Firstly, we invert for the water velocity variation Δv and the tidal height Δz. Secondly, in FWI, we modify the velocity model for each shot point on the fly by adding Δv and Δz in the water layer and reverse the depth change when we calculate the gradient.

We use a synthetic example to illustrate the benefits of Water-Layer Variant FWI. Figure 1a shows the true time-lapse velocity model. A 200 m/s velocity decrease (corresponding to 8% velocity change, indicated by red color) was placed in a 600×100 m anticline structure to simulate a softening reservoir. We then ran FWI for the baseline and monitor using a smooth initial model. As expected, we obtained a clean and localized velocity change for this simple case (Figure 1b). The 4D velocity difference has slight side lobe effects compared to the true difference, which is due to frequency band limitations in FWI. Then we generated the data using the altered water column velocity and thickness. The magnitude of water velocity change was 2 m/s and tidal height is 1 m, which was based on the real water column change during the acquisition of the case study we present below. When we performed conventional FWI, we observed the appearance of 4D noise everywhere (Figure 1c). Although we allowed FWI to update the velocity in the entire section, including the water layer, it failed to correctly tackle the water column changes and these errors leaked to all layers below. The magnitude of the erroneous velocity change was as high as 60 m/s. On the other hand, Water-Layer Variant FWI (Figure 1d) attenuated the 4D noise generated by water column variation well and produced a result almost identical to the simple case in Figure 1b.

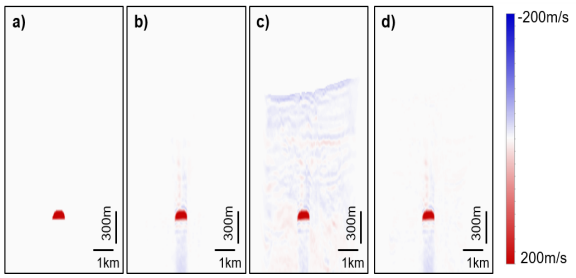

Figure 1: Synthetic test showing 4D velocity difference between (a) True baseline and monitor velocities, (b) FWI of baseline and monitor (no water velocity and tidal height variations in generating the synthetic data), (c) FWI of baseline and monitor (with water velocity and tidal height variations in generating the synthetic data), (d) Water-Layer Variant FWI of baseline and monitor (with water velocity and tidal height variations in generating the synthetic data).

Laverda oil field 4D FWI towed-streamer case study

The Laverda oil field is located offshore of Western Australia, northwest of the Exmouth sub-basin. The field was discovered in October 2000, resulting in the drilling of Laverda-1 that encountered a 72 m oil and gas column in the Late Jurassic to Early Cretaceous Macedon Sandstone. Appraisal programs, including both seismic and wells, were carried out by Woodside in the following years. The seismic was reprocessed in 2018, which generated a 15 Hz FWI model.

The baseline and monitor surveys were acquired by towed-streamer acquisition in 2010 and 2020, respectively, to monitor ongoing production. The acquisitions cover an area of 145 km^2. The baseline has 6 cables with receiver depth of

10.1190/segam2021-3582747.1

7 m and streamer length of 3750 m. The monitor has 10 cables with receiver depth of 15 m or 18 m (to reduce swell noise due to bad weather) and streamer length of 5000 m.
A key advantage of 4D FWI is its limited preprocessing. Just as in standard 4D processing, rigorous QCs are conducted to ensure it is 4D friendly. One important step is 4D binning since the cable length and number of cables are different for both surveys. Inspired by conventional time-lapse processing, we implemented a 4D binning strategy based on shot and receiver locations. After 4D binning, the repeatability for horizontal positioning (x and y) is within reasonable limits: Most traces have a dSdR, sum of distance between sources and distance between receivers, of less than 50 m. However, the different streamer depths are a major source of non-repeatability. In conventional 4D processing, receiver deghosting is applied to both data sets to remove the wavelet difference, followed by redatuming the receivers of both data sets to the surface to remove the datum difference. On the other hand, 4D FWI can naturally handle this as it directly places sources and receivers at the right locations as well as models the ghosts directly.

The 15 Hz FWI model from the 2018 reprocessing was used as the starting model for 4D FWI. Two parallel inversions were conducted for the baseline and monitor data using Water-Layer Variant TLFWI from 4 Hz to 18 Hz. The direct difference of the baseline and monitor 18 Hz FWI velocity models is displayed in Figure 2. The velocity difference properly captured the change in the reservoir, which is mostly a softening effect. The S/N of the velocity difference is high: $\Delta v/v$ in the reservoir is around 2%-2.5%, while most of the background noise is below 0.5%.

The next question is how the velocity models from 4D FWI can be used to improve conventional 4D results. To answer this, we migrated the baseline and monitor data separately using the two FWI velocities.

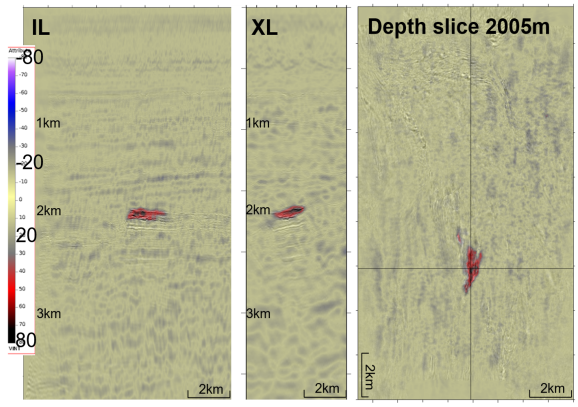

Figure 2: Direct 4D FWI velocity difference shows clear reservoir softening (Overlay on 4D difference of migration stack from conventional 4D production workflow).

The corresponding Kirchhoff PSDM full stacks are shown in Figure 3. In Figures 3a and 3c, as we migrated baseline and monitor with the same velocity, the 4D difference is visible at the bottom of reservoir and below. The 4D difference below the reservoir is 4D noise (blue arrows) generated by kinematic changes at the reservoir. In Figures 3b and 3d, we migrated each vintage with its own velocity, which significantly reduced 4D noise below the reservoirs as expected. This comparison shows that 4D FWI not only provides geologically conformal 4D signal, but also gives a reasonably accurate estimation of velocity changes that more consistently explains both the baseline and monitor data.

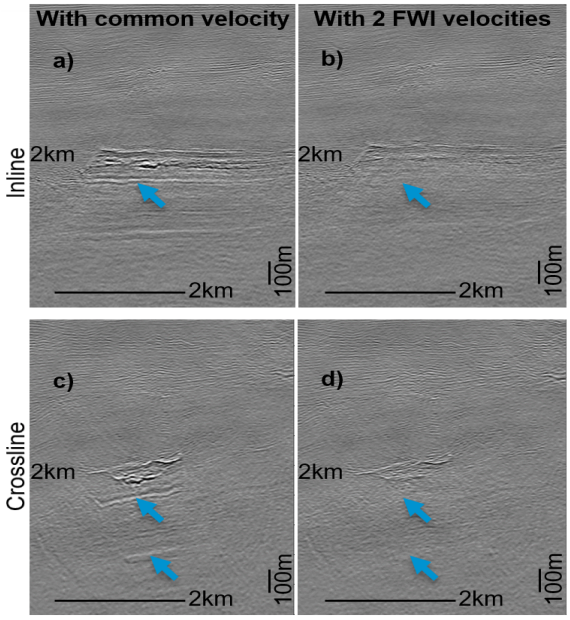

Figure 3: Kirchhoff PSDM full stack 4D difference: Inline views of (a) migration with initial 2018 velocity and (b) migration with separate FWI velocities. Crossline views of (c) migration with initial 2018 velocity and (d) migration with separate FWI velocities.

Next, we checked the impact of 4D FWI on time shift maps. The time shift calculation window length is 500 ms of the under-burden. In Figures 4a, 4c, and 4e, the imprints of the 4D noise stand out from the background due to the overlying reservoir's velocity change. The value and span of time shift anomalies are different from near to far angle stacks, indicating an offset-dependent moveout. Migration with the two FWI velocities attenuated this imprint in the full stack as well as sub-stacks, as shown in Figures 4b, 4d, and 4f.

In conventional 4D processing, an amplitude difference volume and a time shift volume are needed for interpretation. With this new migration result, the amplitude term and time

shift are better decoupled, providing a simplified workflow for 4D interpretation.

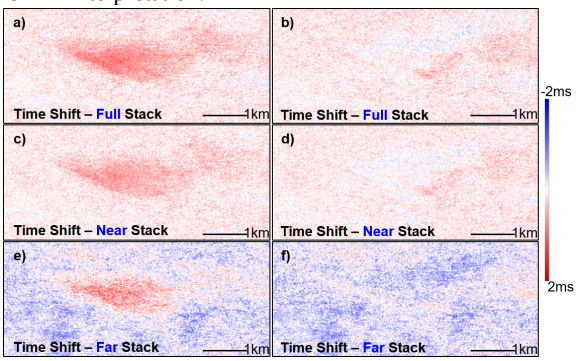

Figure 4: Time shift maps between baseline and monitor for a) Migration full stack with the same initial 2018 velocity; b) Migration full stack with separate FWI velocities; c) Migration near stack with the same initial 2018 velocity; d) Migration near stack with separate FWI velocities; e) Migration far stack with the same initial 2018 velocity; and f) Migration far stack with separate FWI velocities.

Despite a relatively low frequency of the current 4D FWI (18 Hz), we can still spot small-scale reservoir changes in the velocity difference. Figure 5 zooms in on the 4D velocity difference near the Laverda oil field. The reservoir is mostly in red color, showing softening effects caused by overpressure. Meanwhile, we observe that FWI also captures small-scale hardening effects (Figures 5b and 5c). The depth slice (Figure 5a), shows that this hardening effect follows the water injector well path. It demonstrates that the saturation change effect dominates near the well path. Combined with seismic and production history, we believe this could help better understand pressure and saturation changes and better monitor the fluid injection.

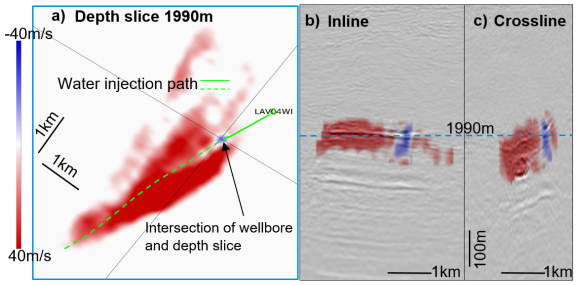

Figure 5: 4D FWI detects hardening effects in an overall softening area (Overlay on 4D difference of migration stack from conventional 4D production workflow).

Another interesting finding was at the survey edge, which is outside our project's main zone of interest. Figure 6 shows the 4D velocity difference extracted onto the top reservoir horizon. An area with hardening effects was found at the northwestern edge with Δv/v around 1.5%-2%. It turns out that this area is the Stybarrow oil field. This oil field started to produce in 2007 and was decommissioned in 2015. Our 4D FWI successfully detected the water sweep between the 2010 and 2015 time period.

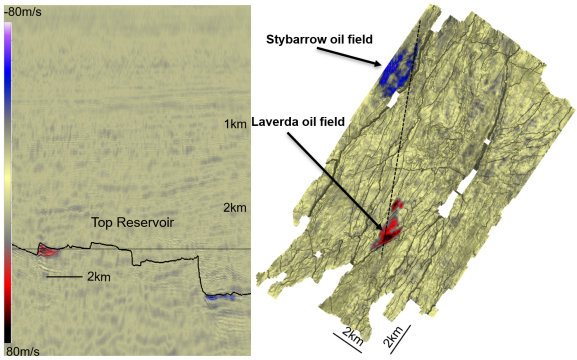

Figure 6: On the left, direct velocity difference in an arbitrary line passing Laverda and Stybarrow oil fields. The top of reservoir horizon is indicated by the black line. 4D difference is confined perfectly by this horizon. On the right, velocity value extracted at the top of reservoir. Stybarrow oil field shows a hardening signal with a good quality even at the edge of the survey.

Conclusions & Discussion

We have proposed a 4D FWI workflow and applied it to a 4D field data set from two towed-streamer surveys in the Exmouth basin. It reliably recovers P-wave velocity changes related to pressure and saturation changes in the reservoir. The observed changes at the reservoir level correlate well with production history. The 4D FWI signal also contains interesting small-scale details showing its potential to provide directly interpretable 4D attributes.

Just like with conventional 4D processing, acquisition repeatability remains a key factor for the success of 4D FWI. Our result was constrained by the repeatability of two towed-streamer acquisitions. And current FWI of baseline and monitor data were independent and only inverted for P-wave velocity. The cross-talk between velocity and other properties (e.g., density) could be a concern. With more repeatable acquisition, like OBS, and continuously improved FWI algorithm, for example using cross-vintage regularization (Maharramov and Biondi, 2014), we believe that 4D FWI can be further improved and will emerge as a valuable reservoir monitoring tool.

Acknowledgments

We thank Woodside, Mitsui E&P Australia Pty Ltd, and CGG for permission to publish this work. We also thank Kai Zhao, Keat Huat Teng, Ping Wang, and Qing Xu for fruitful discussions.

REFERENCES

Hicks, E., H. Hoeber, M. Houbiers, S. P. Lescoffit, A. Ratcliffe, and V. Vinje, 2016, Time-lapse full-waveform inversion as a reservoir-monitoring tool — A North Sea case study: The Leading Edge, **35**, 850–858, doi: https://doi.org/10.1190/tle35100850.1.

Kalinicheva, T., M. Warner, and F. Mancini, 2020, Full-bandwidth FWI: 90th Annual International Meeting, SEG, Expanded Abstracts, 651–655, doi: https://doi.org/10.1190/segam2020-3425522.1.

Kamei, R., and D. Lumley, 2017, Full waveform inversion of repeating seismic events to estimate time-lapse velocity changes: Geophysical Journal International, **209**, 1239–1264, doi: https://doi.org/10.1093/gji/ggx057.

Lailly, P., 1983, The seismic inverse problem as a sequence of before stack migration, *in* J. B. Bednar, R. Redner, E. Robinson, and A. Weglein, eds., Conference on inverse scattering: Theory and application: SIAM, 206–220.

MacBeth, C., M. Mangriotis, and H. Amini, 2018, Review paper: Post-stack 4D seismic time-shifts interpretation and evaluation: Geophysical Prospecting, **67**, 3–31, doi: https://doi.org/10.1111/1365-2478.12688.

Maharramov, M., and B. Biondi, 2014, Joint full-waveform inversion of time-lapse seismic data sets: 84th Annual International Meeting, SEG, Expanded Abstracts, 954–959, doi: https://doi.org/10.1190/segam2014-0962.1.

Maharramov, M., B. Willemsen, P. S. Routh, E. F. Peacock, M. Froneberger, A. P. Robinson, G. W. Bear, and S. K. Lazaratos, 2019, Integrated kinematic time-lapse inversion workflow leveraging full-waveform inversion and machine learning: The Leading Edge, **38**, 943–948, doi: https://doi.org/10.1190/tle38120943.1.

Routh, P., G. Palacharla, I. Chikichev, and S. Lazaratos, 2012, Full wavefield inversion of time-lapse data for improved imaging and reservoir characterization: 82nd Annual International Meeting, SEG, Expanded Abstracts, doi: https://doi.org/10.1190/segam2012-1043.1.

Tarantola, A., 1984, Inversion of seismic reflection data in the acoustic approximation: Geophysics, **49**, 1259–1266, doi: https://doi.org/10.1190/1.1441754.

Wang, P., Z. Zhang, J. Mei, F. Lin, and R. Huang, 2019, Full-waveform inversion for salt: A coming of age: The Leading Edge, **38**, 204–213, doi: https://doi.org/10.1190/tle38030204.1.

Yang, D., M. Meadows, P. Inderwiesen, J. Landa, A. Malcolm, and M. Fehler, 2015, Double-difference waveform inversion: Feasibility and robustness study with pressure data: Geophysics, **80**, no. 6, M129–M141, doi: https://doi.org/10.1190/geo2014-0489.1.

Zhang, Z., J. Mei, F. Lin, R. Huang, and P. Wang, 2018, Correcting for salt misinterpretation with full-waveform inversion: 88th Annual International Meeting, SEG, Expanded Abstracts, 143–1147, doi: https://doi.org/10.1190/segam2018-2997711.1.

Zhang, Z., Z. Wu, Z. Wei, J. Mei, R. Huang, and P. Wang, 2020, FWI Imaging: Full-wavefield imaging through full-waveform inversion: 90th Annual International Meeting, SEG, Expanded Abstracts, 656–660, doi: https://doi.org/10.1190/segam2020-3427858.1.

Zhou, W., and D. Lumley, 2019, Central-difference time-lapse 4D seismic full waveform inversion: 89th Annual International Meeting, SEG, Expanded Abstracts, 5219–5223, doi: https://doi.org/10.1190/segam2019-3213915.1.